OPEN ACCESS
ARTICLE

Effect of the pH Value of Synthesis Conditions on the Phase Structure and Photocatalytic Properties of Bismuth Molybdates Synthesized Using a Hydrothermal Method

Regular Paper

Wenfeng Guo[1,2]*, Heping Li[1], Weixiu Teng[1], Linfan Cui[1] and Tifeng Jiao[1,2,3]*

1 Hebei Key Laboratory of Applied Chemistry, School of Environmental and Chemical Engineering, Yanshan University, Qinhuangdao, P. R. China
2 State Key Laboratory of Metastable Materials Science and Technology, Yanshan University, Qinhuangdao, P. R. China
3 National Key Laboratory of Biochemical Engineering, Institute of Process Engineering, Chinese Academy of Sciences, Beijing, P. R. China
*Corresponding author(s) E-mail: wfguo@ysu.edu.cn; tfjiao@ysu.edu.cn

Received 27 March 2015; Accepted 18 August 2015

DOI: 10.5772/61294

Abstract

Bismuth molybdate single-crystallites were synthesized by a simple hydrothermal method at different pH values. The as-fabricated samples were characterized by X-ray diffraction (XRD) and transmission electron microscopy (TEM); it has been found that the pH values of the precursors can significantly influence the structures of the products. Under the Bi/Mo ratio of 2:1 conditions (a nominal composition of Aurivillius structure), low pH leads to the formation of γ-Bi_2MoO_6 with Aurivillius type structure, while neutral and higher pH values lead to the formation of γ-Bi_2MoO_6/Bi_2O_3 composite, and Bi_2O_3, respectively. The photocatalytic activities of the samples with different structures were measured for the degradation of methylene blue (MB) under simulated sunlight irradiation. Among the as-fabricated bismuth molybdate samples, the γ-Bi_2MoO_6 exhibited superior photocatalytic efficiency to the γ-Bi_2MoO_6/Bi_2O_3 composite and the Bi_2O_3, mainly due to its unique layered Aurivillius structure, smaller band gap structures and smaller particle sizes.

Keywords γ-Bi_2MoO_6, Aurivillius structure, photocatalytic activity, methylene blue (MB), pH values

1. Introduction

Recently, bismuth molybdates have been studied extensively because of their rich microstructures and interesting properties [1-3]. In general, bismuth molybdates have the general chemical formula Bi_2O_3 $nMoO_3$ where n = 3, 2 or 1, corresponding to three structures: α-$Bi_2Mo_3O_{12}$, β-$Bi_2Mo_2O_9$ and γ-Bi_2MoO_6 [1, 4]. As a typical candidate within this family, γ-Bi_2MoO_6 with Aurivillius structure shows great potential to be utilized in solar energy [4-6].

It is well known that the microstructure of materials plays an important role in their physical and chemical properties, and that different microstructures are affected by the methods and conditions of synthesis. Conventionally, bismuth molybdate crystals are synthesized using various synthesis methods, including solid-state reaction [7], sol-gel [8], co-precipitation [9], hydrothermal methods [10], and so on. Among these methods, the hydrothermal route is one of the most effective methods for synthesizing different microstructures of bismuth molybdates. This process can be described as a reaction of precursors in a close system in the presence of a solvent. It is possible to control the structure and morphology of products by adjusting the processing parameters: for instance, using different solvents and reactants, surfactants, pH values, reaction temperatures and times [11-13]. In this paper, bismuth molybdates with the ratio Bi:Mo = 2:1 (a nominal composition of Aurivillius structure) are synthesized by the simple hydrothermal method at various pH values. The influence of pH value on the microstructure, morphology, band gap energy and photocatalytic activities are investigated carefully. The objective of this work is to identify suitable pH value conditions to obtain bismuth molybdate with Aurivillius structure, and to confirm its outstanding photocatalytic activity.

2. Experimental

2.1 Materials

Bismuth nitrate, sodium molybdate, MB, sodium hydroxide, nitric acid and absolute alcohol were provided by Sinopharm Chemical Reagent Co., Ltd. (Shanghai, China). All chemicals were of analytic grade and used without further purification.

2.2 Preparation of the Bismuth Molybdate samples

Bismuth molybdates were prepared by a simple hydrothermal synthesis. First, $Bi(NO_3)_3$ $5H_2O$ (1.947 g) was rapidly dissolved in 10mL nitric acid solution (2 mol/L), under stirring, to form solution A. Then 0.483g Na_2MoO_4 was dissolved in 10ml sodium hydroxide solution (4 mol/L), under stirring, to form solution B. Thirdly, solution B was added dropwise into solution A to form suspension C. The diluted NaOH and HNO_3 solutions were then added to adjust the pH values, which were taken to be 5, 7 and 9. After being vigorously stirred for 30 min, the resulting precursor suspension was transferred into a 50mL-capacity Teflon-lined stainless steel autoclave, which was subsequently heated to 160°C and maintained for 22 h. Subsequently, the autoclave was cooled to room temperature naturally. The obtained samples were filtered, washed several times with deionized water, and dried at 80°C in air.

2.3 Characterization

X-ray powder diffraction (XRD) patterns were recorded on a Bruker D8 ADVANCE X-ray diffractometer (Cu Kα source) at a scan rate of 4°/min, with a 2θ range from 10° to 80°. Transmission electron microscopy (TEM) images were recorded on a JEOL JEM-2010 transmission electron microscope at an accelerating voltage of 200 kV. UV-visible absorption spectra and diffuse reflectance spectra (DRS) were recorded on a Lambda 2500 UV-visible spectrophotometer (Japan Island Ferry).

2.4 Photocatalytic Degradation of MB Experiment

MB was used as a convenient photostable organic molecule to assay photochemical activity of the obtained samples. The prepared bismuth molybdate samples (50 mg) were dispersed into an aqueous solution (100 mL) of MB (10 mg/L^{-1}). The suspension was sonicated for 30 min, followed by stirring in the dark for 120 min to ensure adsorption-desorption equilibrium prior to irradiation. The suspension was then irradiated while stirring, using a 500-W Xe lamp (MAX-302, Asahi Spectra, USA). The initial and final reaction temperatures for the MB solution were measured as 25±3°C, respectively. Samples for analysis were taken from the reaction suspension after different reaction times, and centrifuged at 3500 rpm for 10 min to remove the particles. The MB concentration from the upper clear solution was analysed according to the absorption intensity at 664 nm, within the measured UV-vis spectra. The pH value of the MB solution was about 7.

3. Results and Discussion

3.1 XRD Analysis

Fig. 1 shows the XRD patterns of the samples with the ratio Bi:Mo = 2:1 at various pH values. It can be clearly seen that the XRD patterns of the powders obtained at a pH of 5 can be ascribed to the Aurivillius structure of γ-Bi_2MoO_6. These diffraction peaks are in good agreement with the standard γ-Bi_2MoO_6 sample (ICDD PDF #84-0787). No impurity peaks were observed in any of the XRD patterns, indicating that the sample was pure orthorhombic γ-Bi_2MoO_6. When the pH value was increased to 7, besides γ-Bi_2MoO_6, the cubic Bi_2O_3 fluorite structures were also observed in the XRD patterns of the samples. Indeed, it was mainly the Bi_2O_3 fluorite structure phase that was present when the pH value was increased to 9 [4]. The formation of the Bi_2O_3 phase in the higher pH value conditions should be ascribed to the preference of the metal hydroxide when the pH value is high. In this case, the Bi_2O_3 phase is obtained from its hydroxide in the hydrothermal system. These results indicate that acidic conditions are favourable for the formation of γ-Bi_2MoO_6 with Aurivillius structure.

3.2 TEM Analysis

Fig. 2 shows the TEM images of the as-prepared samples, synthesized by hydrothermal method at different pH values condition. Fig. 2a shows regular morphology and smaller nanospheres or nanotablets (~100 nm) for γ-

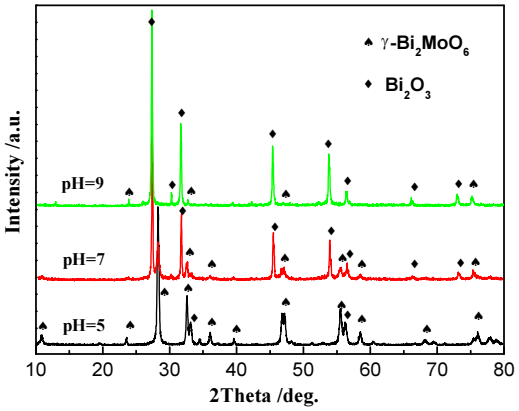

Figure 1. XRD patterns of the samples obtained at different pH values

Bi_2MoO_6 at pH 5. The γ-Bi_2MoO_6/Bi_2O_3 composite nanocrystals obtained at pH 7 are composed of crystals with thinner, conjoined nanosheets, as shown in Fig. 2b. The as-prepared Bi_2O_3 at pH 9 possesses an irregular morphology and the aspect ratio of some of the grains is larger (Fig. 2c). It can be concluded that the pH value of the synthesis conditions dramatically affects the surface morphology of the bismuth molybdates, or Bi_2O_3, during the hydrothermal process. The different surface morphology would then further influence the surface chemistry, charge separation and excited state lifetimes, all of which are closely related to the photocatalytic activity of the materials.

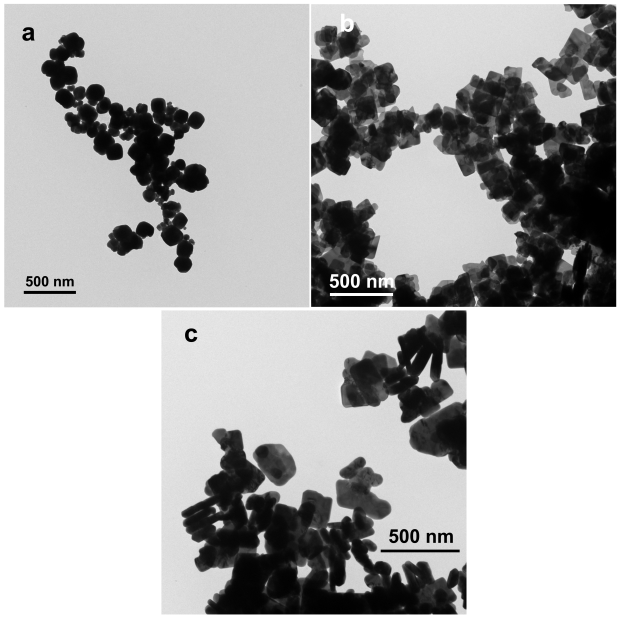

Figure 2. TEM images of the samples obtained at different pH values: (a) pH = 5, (b) pH = 7, (c) pH = 9

3.3 Band gap of Bismuth Molybdate Materials

Fig. 3a shows the UV-visible diffuse reflectance spectra of the bismuth molybdate and Bi_2O_3 samples obtained at different pH value conditions. All of the samples exhibit a strong absorption from ultraviolet light to the visible light region shorter than 500 nm, and a steep shape of the spectra around 500 nm, indicating that the light absorption is not due to impurities in the samples but to the band-gap transition. A slight blue shift of the absorption band edge of the samples can be observed as the pH value increases from 5 to 9; the γ-Bi_2MoO_6 possesses the onset of the absorption edge at the longest wavelength among them. Based on the absorption edge values, the intrinsic band gaps of the crystalline semiconductors could be estimated from the following formula:

$$\alpha E_{\text{photon}} = K\left(E_{photon} - E_g\right)^{1/2}$$

where α is the absorption coefficient, E_{photon} is the discrete photoenergy, K is a constant, and E_g is the band gap energy. The intercept of the tangents to the x-axis can give good approximation of the band gap energy for the products. As shown in Fig. 3b, the estimated band gaps corresponding to the absorption edge values are given in Table 1. The results demonstrate that there is a smaller band gap energy value for γ-Bi_2MoO_6 synthesized at pH=5, which is useful for its photocatalytic activity under sunlight irradiation.

Synthesis conditions	Samples	Absorption edge (nm)	Band gap energy E_g (eV)
pH = 5	γ-Bi_2MoO_6	492	2.52
pH = 7	γ-Bi_2MoO_6/Bi_2O_3	478	2.60
pH = 9	Bi_2O_3	470	2.63

Table 1. Absorption edge and band gap energy of bismuth molybdates for different surfactant nanocrystals

3.4 Photocatalytic Activities

The photocatalytic activities of different bismuth molybdate products were evaluated by the degradation of MB solution upon simulated sunlight irradiation. Fig. 4 shows the time-dependent absorption spectra of MB solution during the photodegradation process in the presence of the three kinds of bismuth molybdates samples. The absorption peaks at 664 nm, corresponding to MB, decreased gradually as the irradiation time was extended. Compared with the absorption peaks of γ-Bi_2MoO_6/Bi_2O_3 and Bi_2O_3, respectively, that of the γ-Bi_2MoO_6 obtained at pH 5 decreased dramatically and completely disappeared after about 90 min. This suggests that γ-Bi_2MoO_6 exhibited the highest photocatalytic activity among the three kinds of bismuth molybdate samples. The variation of MB concentrations (C/C_0) with irradiation time over the different samples was shown in Fig. 5, where C_0 and C are the concentrations of MB solution before and after irradiation, respectively. For comparison, the direct photolysis of MB in the absence of bismuth molybdate was also performed under the same conditions. As shown in Fig. 5, MB concentration in the absence of the catalysts hardly changed with the increase of irradiation time. In contrast, the as-synthesized bismuth molybdate samples, obtained at

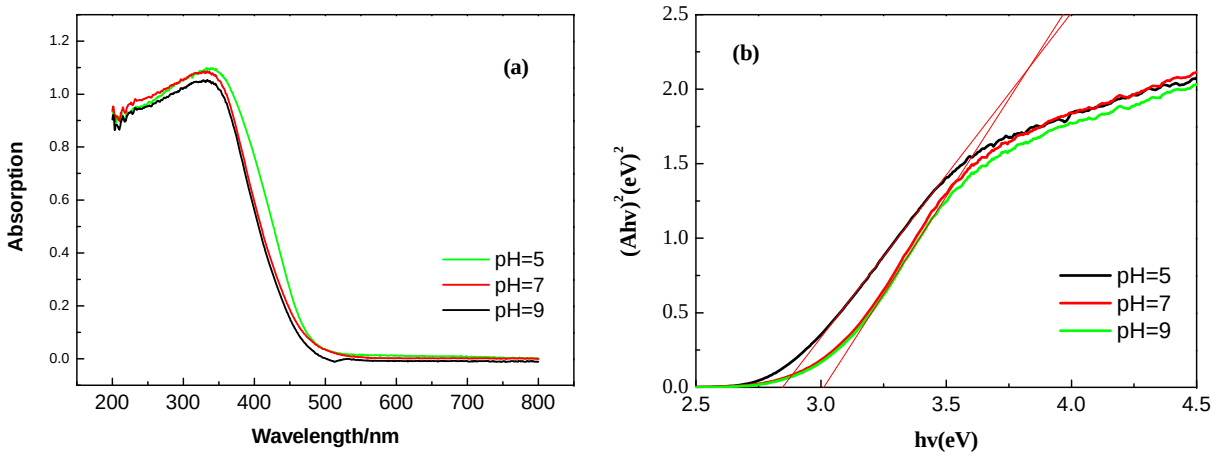

Figure 3. (a) The UV-vis diffuse reflectance spectra and (b) the (ahv)2 versus energy (hv) curve of the samples obtained at different pH values

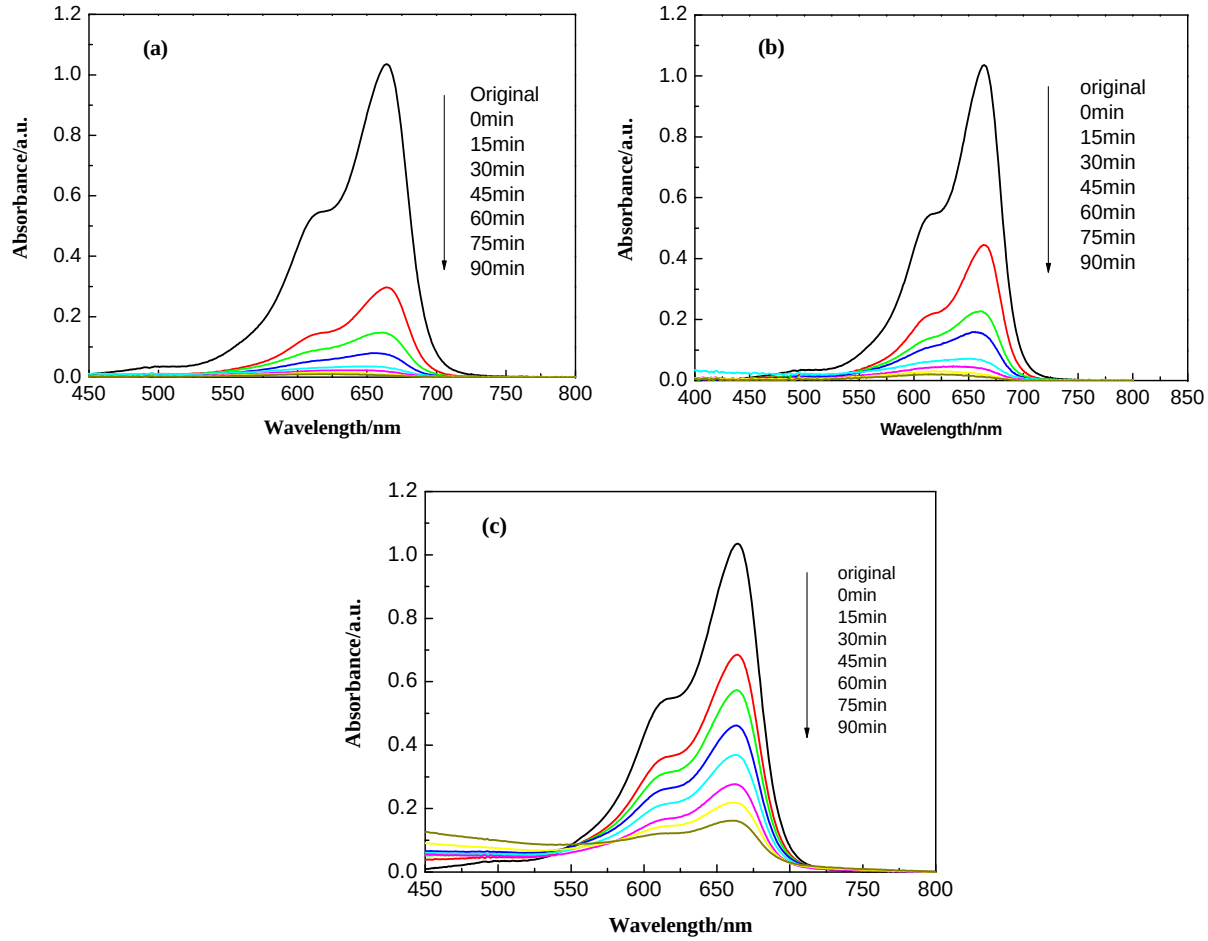

Figure 4. Time-dependent UV-vis absorption spectra of the MB solution in the presence of various photocatalysts: (a) γ-Bi_2MoO_6, (b) γ-Bi_2MoO_6/Bi_2O_3, (c) Bi_2O_3

different pH values condition, exhibited remarkable variation in photocatalytic activities for MB degradation. Among them, the hydrothermally synthesized γ-Bi_2MoO_6 showed the highest photoactivity under simulated sunlight irradiation. The MB photocatalytic degradation rate was up to 97.1 % after 90 min under Xe lamp irradiation. Nevertheless, the photocatalytic activity of the hydrothermally synthesized γ-Bi_2MoO_6/Bi_2O_3 and Bi_2O_3 were significantly lower than that of γ-Bi_2MoO_6: 89.9 % and 75.6 % of the photodegradation rate, respectively.

It is well known that the photocatalytic activity of semiconductor materials is mainly governed by their microstructure, morphology, band gap energy, etc. Firstly, the different photocatalytic activities of the three samples can be attributed to their different microstructures. The γ-

Bi_2MoO_6 with the Aurivillius phase has been found to possess a unique layered structure, in which perovskite slabs of corner-sharing, distorted MoO_6 octahedra are sandwiched between $(Bi_2O_2)^{2+}$ layers [14]. In general, layered structure-type materials have a higher activity under the same conditions, due to the facile migration and separation of photogenerated charges in such a layered structure [15]. On the other hand, the surface morphology also plays a vital role in photocatalytic performance. The γ-Bi_2MoO_6 sample possesses a regular morphology and smaller nanospheres (about 100 nm), which probably gives it a specific surface chemistry, efficient charge separation and longer excited state lifetimes. This also leads to the higher photocatalytic efficiency and better photocatalytic activity for γ-Bi_2MoO_6. Another reason for the high activity is the smaller band gap (2.59 eV) of the γ-Bi_2MoO_6, which responds to the onset of the absorption edge at the longer wavelength. The amount of photons absorbed by photocatalysts with smaller band gaps is larger than that absorbed by photocatalysts with larger band gaps [16]. Therefore, the superior activity of γ-Bi_2MoO_6 might be ascribed to its smaller band gap.

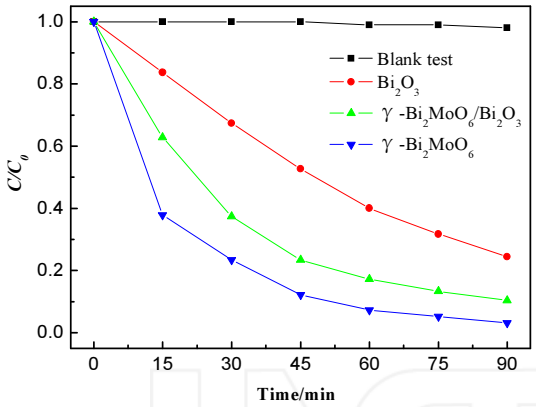

Figure 5. Photocatalytic degradation of MB versus simulated sunlight irradiation time for the different photocatalysts used

4. Conclusion

In summary, bismuth molybdate materials were prepared using a facile hydrothermal method by controlling Bi/Mo ratio and pH values. It was found that different pH values resulted in distinctly different crystalline phases, surface morphologies and band gaps. Of these, γ-Bi_2MoO_6 with an Aurivillius structure, specific morphology and smaller band gap was obtained under acidic conditions, and exhibited an excellent photocatalytic activity in the decomposition of MB under simulated sunlight irradiation.

5. Acknowledgements

This work was financially supported by the National Natural Science Foundation of China (Nos. 21473153 and 61275100), the Natural Science Foundation of Hebei Province (No. B2013203108), the Science Foundation for the Excellent Youth Scholars from Universities and Colleges of Hebei Province (No. YQ2013026), the Support Program for the Top Young Talents of Hebei Province, and the Open Foundation of the National Key Laboratory of Biochemical Engineering (Institute of Process Engineering, Chinese Academy of Sciences).

6. References

[1] Reilly L M, Sankar G, Catlow C R A (1999) Following the Formation of γ-Phase Bi_2MoO_6 Catalyst by in Situ XRD/XAS and Thermogravimetric Techniques. J. Solid State Chem. 148: 178-185.

[2] Sim L T, Lee C K, West A R (2002) High oxide ion conductivity in Bi_2MoO_6 oxidation catalyst. J. Mater. Chem. 12: 17-19.

[3] Marinova V, Veleva M (2002) Refractive index measurements and transmission spectra of $Bi_2(MoO_4)_3$ single crystals. Opt. Mater. 19: 329-333.

[4] Kongmark C, Coulter R, Cristol S, Rubbens A, Pirovano C, Löfberg A, Sankar G, van Beek W, Bordes-Richard E, Vannier R-N (2012) A Comprehensive Scenario of the Crystal Growth of γ-Bi2MoO6 Catalyst during Hydrothermal Synthesis. Cryst. Growth Des. 12: 5994-6003.

[5] Kubacka A, Fernández-García M, Colón G (2012) Advanced Nanoarchitectures for Solar Photocatalytic Applications. Chem. Rev. 112: 1555-1614.

[6] López Cuéllar E, Martínez-de la Cruz A, Lozano Rodríguez K H, Ortiz Méndez U (2012) Preparation of γ-Bi_2MoO_6 thin films by thermal evaporation deposition and characterization for photocatalytic applications. Catal. Today 166: 140-145.

[7] Rastogi R P, Singh A K, Shukla C S (1982) Kinetics and mechanism of solid-state reaction between bismuth(III) oxide and molybdenum(VI) oxide. J. Solid State Chem. 42: 136-148.

[8] Le M T, Bac L H, Van Driessche I, Hoste S, Van Well W J M (2008) The synergy effect between gamma and beta phase of bismuth molybdate catalysts: Is there any relation between conductivity and catalytic activity? Catal. Today. 131: 566-571.

[9] Martínez-de la Cruz A, Obregón Alfaro S (2010) Synthesis and characterization of γ-Bi_2MoO_6 prepared by co-precipitation: Photoassisted degradation of organic dyes under vis-irradiation. J. Mol. Catal. A: Chem. 320: 85-91.

[10] Zhang L, Xu T, Zhao X, Zhu Y (2010) Controllable synthesis of Bi_2MoO_6 and effect of morphology and variation in local structure on photocatalytic activities. Appl. Catal. B: Environ. 98: 138-146.

[11] Lin X, Li H, Yu L, Zhao H, Yan Y, Liu C, Zhai H (2013). Efficient removal rhodamine B over hydrothermally synthesized fishbone like $BiVO_4$. Mater. Res. Bull. 48: 4424-4429.

[12] Zhang L, Wang H, Chen Z, Wong P K, Liu J (2011) Bi_2WO_6 micro/nano-structures: Synthesis, modifi-

cations and visible-light-driven photocatalytic applications. Appl. Catal. B: Environ. 106: 1-13.

[13] Yang T, Xia D, Chen G, Chen Y (2009) Influence of the surfactant and temperature on the morphology and physico-chemical properties of hydrothermally synthesized composite oxide $BiVO_4$. Mater. Chem. Phys. 114: 69-72.

[14] Ricote J, Pardo L, Castro A, Millán P (2001) Study of the Process of Mechanochemical Activation to Obtain Aurivillius Oxides with n = 1. J. Solid State Chem. 160: 54-61.

[15] Takata T, Tanaka A, Hara M, Kondo J N, Domen K (1998) Recent progress of photocatalysts for overall water splitting. Catal. Today. 44: 17-26.

[16] Kato H, Kudo A (2001) Energy structure and photocatalytic activity for water splitting of $Sr_2(Ta_{1-x}Nb_x)_2O_7$ solid solution. J. Photochem. Photobiol. A. 145: 129-133.